applied sciences

MDPI

Article

A Novel Way of Optimizing Headlight Distributions Based on Real Life Traffic and Eye Tracking Data *Part 1: Idealized Baseline Distribution*

Jonas Kobbert [1], Anil Erkan [2,*], John D. Bullough [3] and Tran Quoc Khanh [2]

[1] AUDI AG, Auto-Union-Str. 1, 85057 Ingolstadt, Germany; jonas.kobbert@audi.de
[2] Laboratory of Adaptive Lighting Systems and Visual Processing, Technical University of Darmstadt, Hochschulstr. 4a, 64289 Darmstadt, Germany; khanh@lichttechnik.tu-darmstadt.de
[3] Icahn School of Medicine at Mount Sinai, Light and Health Research Center, Population Health Science and Policy, 150 Broadway, Suite 560, Albany, NY 12204, USA; john.bullough@mountsinai.org
* Correspondence: erkan@lichttechnik.tu-darmstadt.de; Tel.: +49-6151-16-22884

Abstract: In order to find optimized headlight distributions based on real traffic data, a three-step approach is chosen. Since the complete investigations are too extensive to fit into a single publication, this paper is the first in a series of three publications. Over three papers, a novel way to optimize automotive headlight distributions based on real-life traffic and eye-tracking data is presented, based on 119 test subjects who participated in over 15,000 km of driving, including recordings of gaze behavior, light data, detection distances, and other objects in traffic. In the present paper, a baseline headlight distribution is derived from a series of detection tests conducted under ideal conditions, with a total of three tests, each with 19–30 subjects, conducted within the same test environment. In the first test, the influence of low beam intensity on the detection of pedestrians on the sidewalk (5.0 m from the center of the driving lane) is investigated. In the second test, the influence of different high beam intensities was investigated for the same detection task. In the third test, the headlight distribution and intensity are kept constant at a representative high beam level, but the detection task is changed. In this test, the pedestrian detection target is placed along different detection angles, ranging from immediately adjacent to the road (2.5°) to 15.5 m away from the center of the driving lane (8.0°). As mentioned, all of these tests were conducted under ideal conditions, with the studies taking place on an airfield with a 1.2 km long straight road and normal road markings, but without oncoming traffic, tasks other than keeping the vehicle with cruise control within its lane, or other distracting objects present. The tests yielded two sets of data; the first is the intensity, based on the first two studies, needed to ensure sufficient intensity to detect objects under ideal conditions at distances needed for different driving speeds. The last test then uses these intensities and necessary variations in the required intensity to create an idealized, symmetric headlight distribution as a baseline for subsequent publications. Although the distribution applies only to passenger vehicles like the one used in the test, the same approach could be applied to other vehicle types. The second paper of this series will focus on real traffic objects and their distributions within the traffic space in order to identify relevant areas in headlight distribution when driving under real traffic conditions. The third paper of this series will analyze driver gaze distributions during real driving scenarios. The data from all three papers are used to create optimized headlight distributions, thereby showing how such an optimized distribution relates to current headlight distributions in terms of luminous flux, intensity, and overall distribution.

Keywords: automotive lighting; adaptive driving beam; light distributions; eye tracking; gaze distributions; pedestrian; detection; laser headlamps

Citation: Kobbert, J.; Erkan, A.; Bullough, J.D.; Khanh, T.Q. A Novel Way of Optimizing Headlight Distributions Based on Real Life Traffic and Eye Tracking Data *Part 1: Idealized Baseline Distribution*. *Appl. Sci.* **2023**, *13*, 9908. https://doi.org/10.3390/app13179908

Academic Editor: Andrés Márquez

Received: 11 April 2023
Revised: 29 August 2023
Accepted: 30 August 2023
Published: 1 September 2023

1. Introduction

In recent decades, automotive headlight technology has evolved drastically. Starting with tungsten halogen headlamps, high-intensity discharge light sources were introduced in the 1990s, increasing the light output significantly from 1500 lm to 3200 lm, while at the same time having a much "cooler" (bluer) light appearance that further increased brightness perception for drivers Bullough [1]. Light-emitting diodes (LEDs), which followed shortly after in the early 2000s, brought much-needed flexibility for the creation of smaller, more attractive headlamps, but also offered the possibility of new functions, such as the adaptive driving beam (ADB), without adding moving parts to the headlamp. Laser light sources and millions of individually addressable pixels, in the form of digital mirror device (DMD) technology, followed soon after in vehicular lighting systems.

However, the main headlight distributions, passing (low) beam and driving (high) beam, have remained largely unchanged when it comes to the actual distribution of light. While there has been a significant amount of research available in this regard, due to the technology available at the time, many compromises were needed to develop the requirements for these functions.

Studies by DIEM, DAMASKY, HUHN, LOCHER, and KLEINKES [2–7] have investigated the necessary contrast, eye movement, required luminous intensity under different adverse conditions, and preferred homogeneity within different parts of the headlight distribution. However, not only have available research techniques changed drastically with improved computing power and eye tracking technology, but the traffic situation has also changed for drivers. Furthermore, with the availability of light sources such as LEDs and lasers, possibilities for optimizing headlight distributions in terms of homogeneity and intensity have changed drastically. Numerous investigations have occurred in recent years regarding the visibility requirements from advanced headlight systems and illumination requirements for visibility and visually guided behavior at night MÜLLER, ROSENHAHN, KANNA, ERKAN, REAGAN, FUNK, WALDNER, CENGIZ, WINTER [8–18] While MOISEL has proposed some initial optimizations [19], the present series of papers will go into further detail.

The UN ECE regulations currently allow four different passing beam distributions [20]: for country roads, urban roads, motorways, and adverse weather conditions. It is conceivable that many more situations exist, under which optimized headlight distributions may lead to benefits for the driver. Depending on road curvature, the number and width of lanes, weather, traffic, driving speed, and the presence of glare sources and other objects within the general traffic space, the possibility of automatically optimizing and generating different light distributions could lead to significant safety improvements for driving at night.

For this reason, the following studies will focus on the required intensity from low and high beams to enable safe detection of obstacles for drivers. From these studies, an idealized headlight distribution for driving under ideal conditions such as those used in this study—a completely straight road with no distraction, such as other cars and lights—is derived. The subsequent publications in this series will focus on modifying this distribution for different real-world conditions.

Investigations

In the following sections, the three main studies are presented. Each part will start by describing the test set-up, the test method, and the test subjects before discussing the results. As mentioned above, the first part will show the variation in passing beam intensity, the second part will focus on driving beam intensity, and the last part will show the influence of different detection angles.

2. Influence of Passing (Low) Beam Intensity on Detection Distances

In order to understand the influence of low beam intensity on the detection of pedestrians and other objects along the road, a test set-up was derived comparable to what ZYDEK, SPRUTE, GIBBONS and others have used [21–23].

2.1. Test Set-Up

The test set-up is located on an empty airstrip with a 1.2 km long straight road. On this road, two human-shaped dummies are placed at a distance of 5 m from the center of each driving lane. Both dummies are coated in a matte black paint with a measured reflectance of ρ = 5%. During each test run, only one of the dummies is shown to the test subjects.

The test vehicle (passenger vehicle) is equipped with modified headlamps that allow pulse-width modulation (PWM) dimming of the passing beam in two stable states. Before the test, both light distributions are measured using a goniophotometer and compared to each other. One passing beam set-up corresponds to a maximum of 21,000 cd (full output), and the other reaches 10,000 cd (50% output). The rest of the light distribution is scaled proportionally.

Both the test vehicle as well as the detection dummies are equipped with GPS sensors, continuously registering their corresponding positions at 5 Hz. The test vehicle is equipped with a detection button. While driving along the straight road at $v_{\text{Test}} = 50\,\text{km}\,\text{h}^{-1}$ (with activated cruise control), the test subjects are then asked to press the button as soon as they are certain that they are able to detect the pedestrian alongside the road. When the button is activated, the current GPS position of the test vehicle is recorded, and the distance to the test dummy's corresponding GPS position can be calculated. This allows measurement of the detection distance to the target.

The complete set-up is shown schematically in Figure 1, where the start of the test is marked by *A*, and the end of the runway is marked by *B*. The dashed gray line indicates the route test subjects took to return to their starting position.

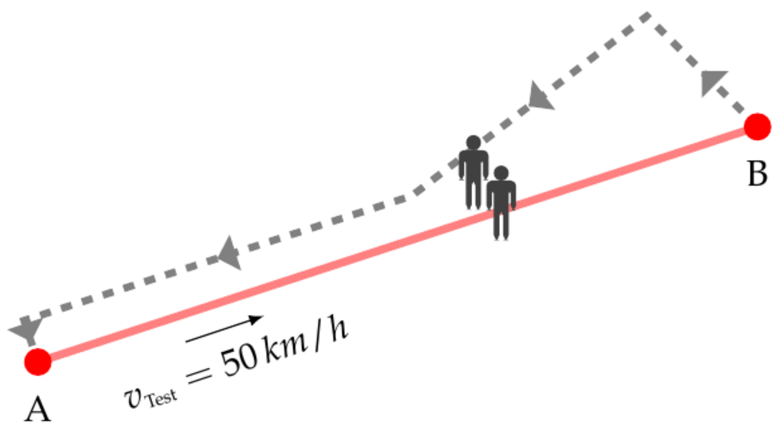

Figure 1. Schematic test set-up for the study on the influence of low beam intensity. The human-like figures indicate possible positions of the detection targets. *A* marks the starting position for the test subjects, and *B* marks the end of the test runway. The dashed gray line is the route used to return from *B* to *A* after a test run to avoid seeing changes in the set-up for the next trial.

To allow proper adaptation to each headlight distribution, the switch between both set-ups is always done at point *B*, so that the subjects can adapt to the new intensity on their way to the starting point (*A*). All test runs are started after dark, when the measured horizontal illuminance on the road is below 0.2 lx.

2.2. Test Subjects

In this test, 19 test subjects, with a mean age of 28 years (range of 23 to 34 years) participated. All subjects were either students or had an office job at the time of the study. This narrow age distribution was chosen specifically to minimize the influence of age in the results. Multiple previous studies [12,14,17,18,23,24] with similar objectives to the present study have used approximately the same or fewer experimental participants as the number used in this part of the study (n = 19).

All test subjects had active drivers' licenses and were invited to participate using their required corrective lenses, if necessary.

2.2.1. Results

The mean measured detection distance for the full low beam was 62.8 m and was 52.6 m for the dimmed low beam. If the reaction time were taken out of this equation, assuming a reaction time of 500 ms Bullough [24], both mean detection distances would be 7 m longer. Both data sets, as seen in Figure 2, follow a normal distribution.

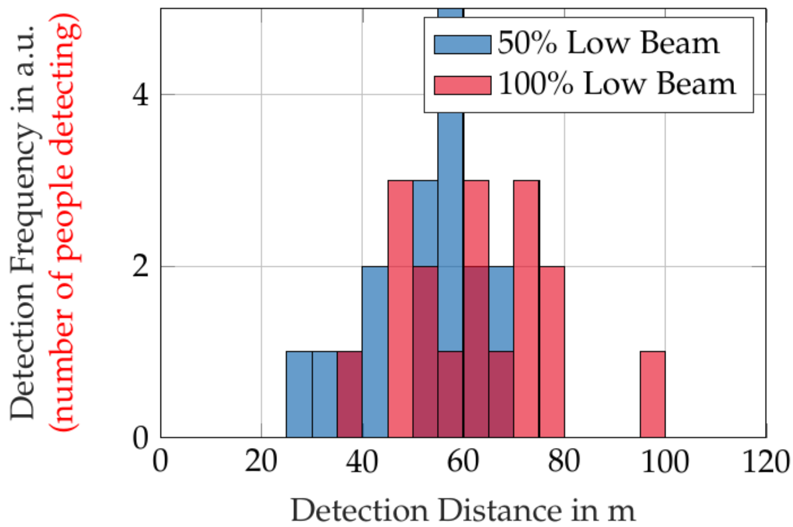

Figure 2. Histogram of the detection distances using 50% low beam (blue) and 100% low beam (red) intensity.

Both headlight conditions represented in Figure 2 illustrate similar variations around the mean, which could be caused by differences in the immediate background around the test dummies, resulting in different contrasts and therefore in different detection distances. Nonetheless, there is little overall difference between the full and dimmed low beam conditions. A two-sample Kolmogorov–Smirnov test shows that the distances for each headlight condition were not significantly different, with $p = 0.08$ being the probability of rejecting the null hypothesis in error. However, a slight trend could be assumed from this data, given the expected longer detection distance found with the full-output low beam.

2.3. Discussion

While dimming the low beam by 50% might lead to the assumption that a detection distance reduction of 75% based on the inverse-square law would be reasonable, this only shows that the low beam intensity is not the primary factor for detecting objects other than the road. Due to the cut-off line separating a high-intensity region below the horizontal from a lower-intensity region above the horizontal and the required vertical aim of headlights (-1% in Europe), the test subjects detect the objects—in this case, pedestrians—so close to the vehicle that the cut-off line seems to be the more salient feature for object detection to ensure enough light and contrast to see the pedestrian target Hecht [25].

Further discussion of these results will follow at the end of this paper, after the other two studies have been presented.

3. Influence of Driving (High) Beam Intensity on Detection Distances

In the next part, the influence of varying high beam intensity on detection distances is tested.

3.1. Test Set-Up

The test set-up is very similar to that used for the passing beam investigation. However, since the use of a high-power high beam in this part was expected to yield much longer detection distances, the test set-up was slightly modified, as shown in Figure 3. Instead of using one detection dummy, a total of five detection dummies were used so that the subjects would have to be certain that they detected the target when pressing the button and were not simply responding quickly based on an anticipated location. Again, the same test dummies were used, and only one dummy was visible during each run.

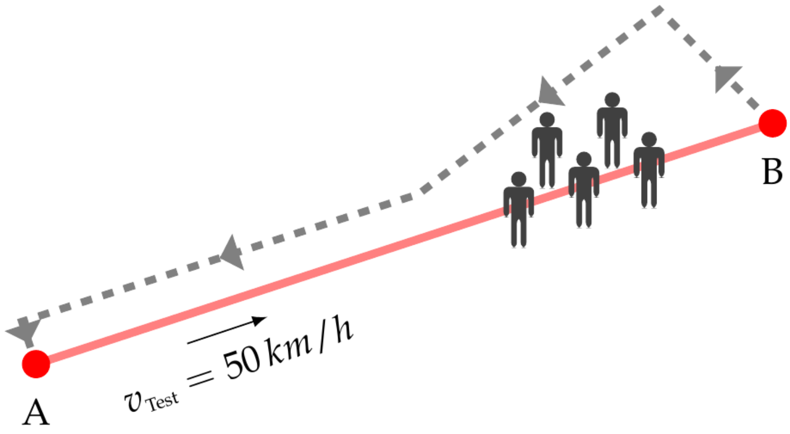

Figure 3. Schematic test set-up to investigate the influence of driving beam intensity on detection distances.

The test vehicle also had to be changed in order to utilize the maximum intensity in the driving beam. For this reason, a BMW i8 with laser headlamps is used for this test. Three different light distributions are investigated in this test: a passing beam (20,000 cd maximum), an LED driving beam (75,000 cd, representing the maximum permitted by the Federal Motor Vehicle Safety Standards [FMVSS] in the U.S.), and an LED driving beam with an additional laser spot designed to create a region of substantially higher intensity in the center of the light distribution (215,000 cd maximum, representing the maximum allowed by UN ECE and Chinese regulations).

Again, all test runs started after the measured horizontal illuminance on the road was below 0.2 lx. The rest of the test set-up, including methods and equipment, was identical to the first test, whereby subjects pressed a button upon detecting the target, allowing the detection distances to be measured by comparing the GPS position of the test car upon detection to the GPS position of the test dummy.

3.2. Test Subjects

In this part, a total of 30 test subjects participated. Twenty-four belonged into the same age group as the test subjects from the passing beam test. Another 6 participants were in an "older" group, with ages between 55 and 65 years. This second age group was included to check the influence of age on detection distances and is not discussed further in this paper. All data presented henceforth are only for the test group between 25 and 35 years of age.

Again, all subjects were either students or worked at an office job at the time of the study. All test subjects were in possession of a driver's license and any required corrective lenses were worn.

3.3. Results

The mean detection distances were 48.2 m for the passing beam and 107.0 m for the (U.S.) driving beam. Adding the laser booster to the driving beam led to a mean distance of 167.4 m, as shown by the data in Figure 4, where the detection distances are grouped into 5 m bins for a detection histogram. All three data sets followed a normal distribution. Two-sample Kolmogorov–Smirnov tests show that all the data sets are significantly different from each other, with the highest p-value being 3.7×10^{-20} for the test between the driving beam and driving beam with the laser spot.

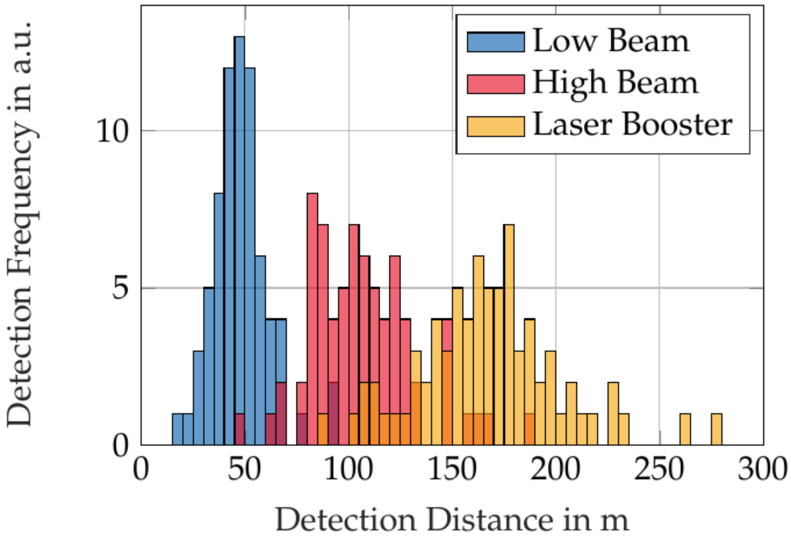

Figure 4. Detection distances for three headlight distributions. Passing beam is shown in blue, driving beam in red, and driving beam with the added laser spot in yellow.

This result is consistent with the relatively small overlap in the distributions of detection distances shown in Figure 4 for each lighting condition. This is true even though each condition exhibits a non-negligible amount of variation. As mentioned previously (Section 2.2.1), this variation is likely caused by differences in contrast between the test dummies and their backgrounds.

3.4. Discussion

Using a passing beam with similar light distribution as in the initial test should have led to the same mean detection distance. However, the test vehicles had slightly different headlight mounting heights. The BMW i8 is a sports vehicle, while the test vehicle in the passing beam test was a "normal" sedan. Since the mounting height of the headlamps is therefore significantly different, and since the first study already showed that the cut-off line and the aiming rather than the intensity was the main influence for detection with the passing beam, this result is explained here.

Increasing the high beam intensity now has the desired effect, and the mean detection distance scales nearly perfectly with the increase in the intensity, since a 3x increase in the maximum intensity should lead to a $\sqrt{3}$ times longer detection distance. Starting with a 107 m detection distance with normal driving beams, this would lead to a 185 m detection distance with the added laser spot. Accounting for the different projected object sizes explains the difference here.

Further discussion will follow at the end of the paper.

4. Light Distribution Intensities

With the data acquired in the first two tests, the next step is to calculate the required luminous intensity for different driving velocities. This can be done using the simple Equation (1) Greibe [26]:

$$s = \frac{\frac{v}{10} \cdot \frac{v}{10}}{2} \tag{1}$$

This equation does not explicitly include any reaction times for the drivers. Since the tests were designed using the detection button described above, the detection time is already subtracted from our detection distances and does not need to be reconsidered. However, it is not as simple as taking the mean detection distances presented in, e.g., Figures 2 and 4, and calculating the maximum velocities that would be possible with those distances.

First of all, the data always refer to mean detection distances, meaning that at the presented distances, only 50% of the test subjects are able to detect the object along the road. For a safe headlight design, this is obviously insufficient. For this reason, the data were recalculated for at least a 95% detection probability. Doing this led to a reduction in the mean detection distances by about 46%, leading to mean detection distances of 36.9 m for low beam (100%), 68.0 m for normal high beam (75,000 cd), and 107.1 m for high beam with the added laser spot (215,000 cd).

Further, two additional factors should be considered. Due to the test being set on an enclosed road, the detection distances could be reduced by a factor of at least $\sqrt{2}$ [27]. On top of that, Bremond shows that the use of a flat detection object, as is the case in the present studies, leads to an increase in detection distances by at least 3.2% [28].

Using these factors, the low beam detection distance is recalculated to be as low as 25.3 m in the real world. The standard high beam now comes down to 46.5 m, and adding the laser spot leads to a 73.0 m detection distance.

Using these data, and accounting for two headlamps in a car, which approximately doubles the available maximum luminous intensity in the hot spot, Figure 5 shows the required luminous intensity over different possible driving speeds. This figure shows that, as the driving speed increases, especially above 100 km h^{-1}, the intensity required to detect pedestrians increases very rapidly.

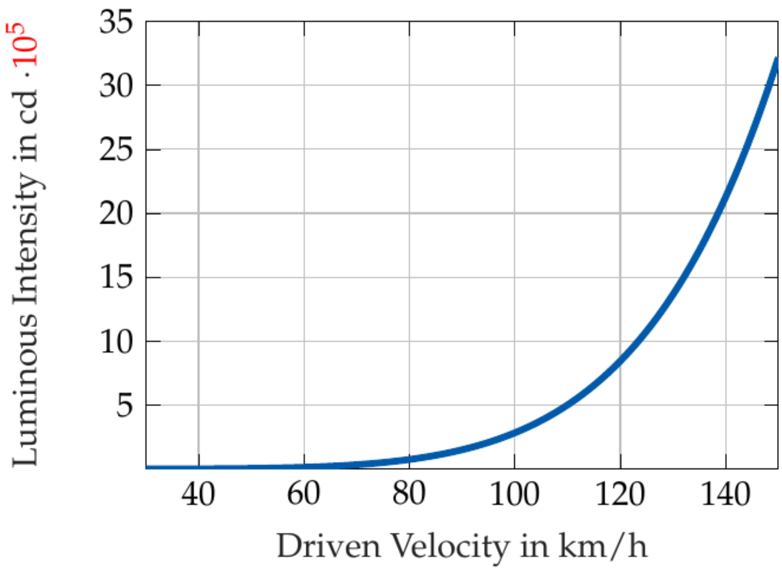

Figure 5. Required luminous intensity for safe object detection under different velocities.

5. Influence of Detection Angles on Detection Distances

After investigating the influence of passing and driving beam intensity in the center of the road, and extracting from these data the required luminous intensity for safe detection, the last part of this paper focuses on the effect of different detection angles by placing the detection objects at different distances from the sides of the road.

5.1. Test Set-Up

Since the main goal in this study is the same as in the previously mentioned studies, the test set-up is kept fairly similar again. The major difference here is that now, instead of aligning the detection dummies along the road, they have been split into different locations. This is schematically shown in Figure 6. Only dummies on the right side of the road are evaluated in this study. Dummies No. 5 and No. 6 are only used to avoid situations where subjects only look for the dummies on the right side of the road. The positions chosen are 2.65, 5.0, 6.5, and 8.0° calculated from the detection distances from the previous study. This leads to positions for the dummies at 5.0, 9.6, 12.5, and 15.5 m from the center of the driving line. These detection angles will of course vary according to the detection distance for each subject individually. This is calculated based on each subject's actual detection distance and the location of the detected target and is presented in the next subsection.

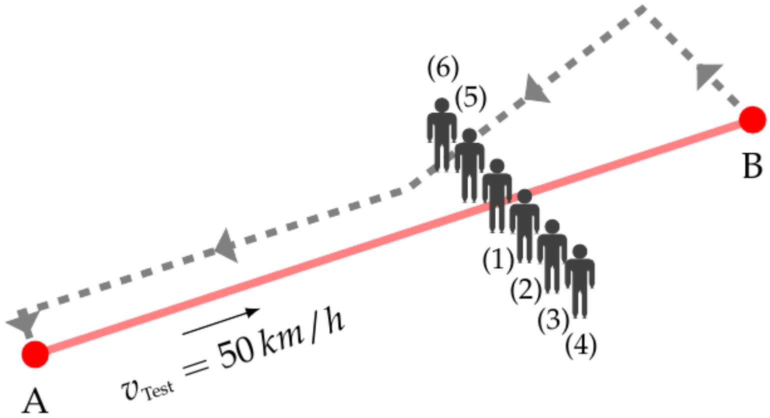

Figure 6. Schematic test set-up to investigate the influence of different detection angles on detection distances. The test dummies are placed at 5.0, 9.6, 12.5, and 15.5 m from the center of the driving lane.

One further difference from the previous tests is that another car was parked at point C. This car was turned off, and all lights were shut off as well. This was done so that the reflection from the lights on the test vehicle coming from the license plate as well as from the rear reflectors was visible, and the test subjects were asked to focus their gaze on these small reflections. This was done to keep the detection angle as consistent as possible. All test runs started after the measured horizontal illuminance on the road was below 0.2 lx.

5.2. Test Subjects

Similar to the previous test, 30 test subjects participated in this test. Again, two age groups were tested. Twenty-two of the participants belong to the same age group as shown for the two previous studies (25–35 years old), and again, only this group's data are shown here. Again, all test subjects were either students or working in an office environment. All test subjects had a valid driver's license and wore any required corrective lenses during the test.

5.3. Results

As mentioned, the actual detection angles would not be the same as assumed prior to the study, since the positions of the detection dummies were fixed and since the detection distance would change from one subject to another. Figure 7 therefore shows the calculated detection angles for each dummy location for all test subjects and test runs. Angles were calculated by taking the arctangent of the ratio between the dummy's lateral offset distance from the center of the driving lane and the detection distance to the dummy.

As shown, a single dummy position can, due to the vastly different detection distances among the test subjects, also lead to different detection angles. The mean detection angles are 3.2, 6.1, 7.8, and 10.5°. As an example, the dummy furthest away from the road (10.5°) is responsible for detection angles between 7° and 15°.

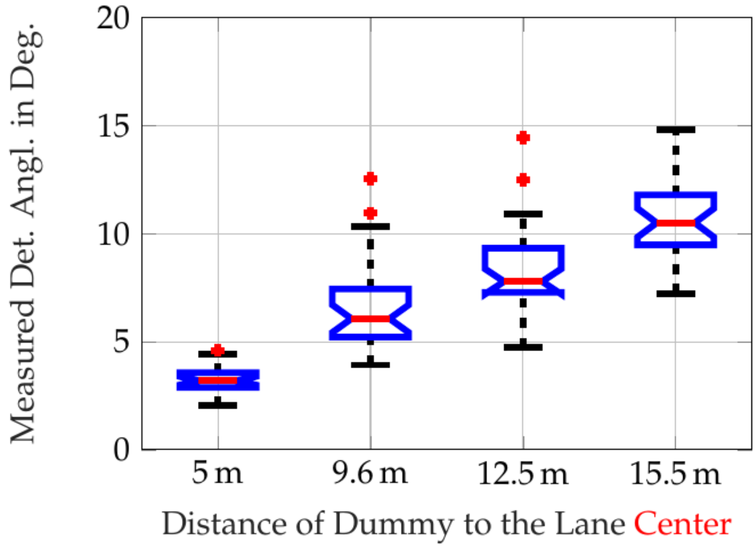

Figure 7. Calculated detection angles for the measured detection distances for all test subjects over the given target positions of 5.0 m (3.2°), 9.6 m (6.1°), 12.5 m (7.8°), and 15.5 m (10.5°). The red bars show the mean distances. The blue bars indicate 50% of all data. The black bars show the range of normal distributed data. Red data points were classified as outliers.

The detection distances were measured as 93.5, 95.5, 97.9, and 84.1 m for the corresponding dummy positions 5.0 m (3.2°), 9.6 m (6.1°), 12.5 m (7.8°), and 15.5 m (10.5°). It is directly obvious that the detection distances remain fairly consistent over the central positions. Even if detection distances at angles smaller than 3.2° had been measured and were much longer than at angles of 3.2° or larger, this would imply that a lower intensity would be needed to detect objects at these small angles. Higher intensities would still support detection of these objects. However, this seems unlikely given the very small differences in detection distances between 3.2° and 7.8°. However, due to the nature of automotive headlight distributions, the light output from headlights at larger detection angles is far lower than immediately adjacent to the road, where, within a few degrees of the line of sight in the parafoveal region of the retina, the targets were more or less viewed on-axis with little change expected in the required intensity. The dummy on the outside therefore has the lowest detection distance due to the least amount of light reaching the dummy under this angle.

Since the absolute detection distances are not the focus of this part of the study, but rather the relative required luminous intensity compared to the center of the light distribution, the luminance at each test dummy was measured for these detection distances. From this, using Equation (2), the illuminance required for the detection angles can be calculated as:

$$I = E \cdot r^2 \text{ and } L = \frac{\rho}{\pi} \cdot E \tag{2}$$

which follows:

$$I = \frac{L \cdot \pi}{\rho} \cdot r^2. \tag{3}$$

Based on this analysis, the required luminous intensities were calculated as follows: 154,453 cd, 76,787 cd, 67,240 cd, and 39,551 cd for the corresponding detection angles. Figure 8 shows these data interpolated in blue and normalized to a value of 1. Extrapolated from this are the data for the left side of the road, assuming a similar relationship between angle and intensity as along the right side.

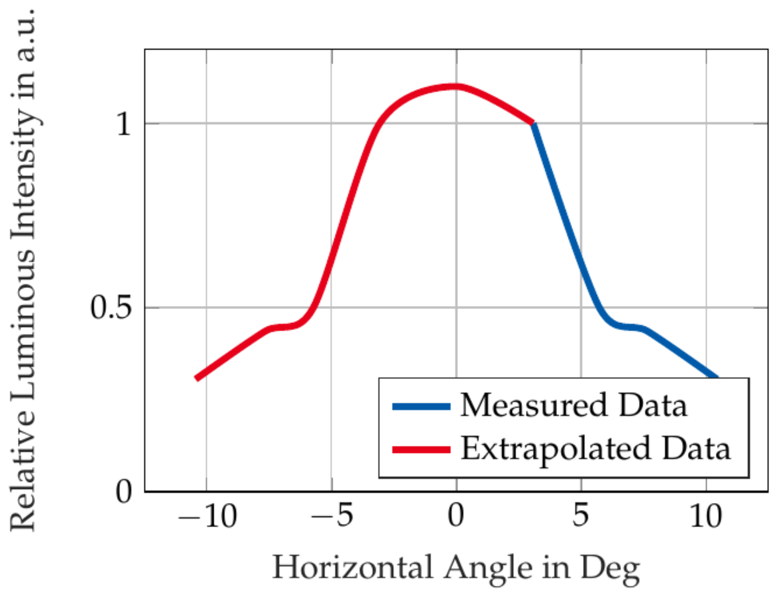

Figure 8. The required normalized luminous intensity for objects under different detection angles: measured (blue) and extrapolated (red) data, assuming the same requirements for objects on the left side of the road as on the right.

These data will now represent the baseline headlight distribution. The horizontal data were taken directly from the data in Figure 8. For the vertical distribution, a Gaussian distribution is added that extends the vertical range of this distribution to have 10% intensity at ±5°, which is standard in current headlights. The resulting baseline headlight distribution is shown in Figure 9.

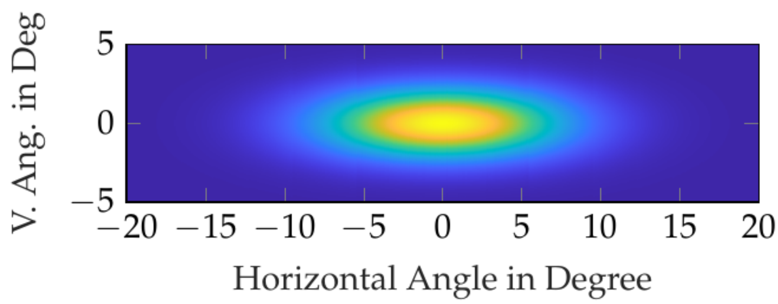

Figure 9. Proposed baseline headlight distribution for the data presented in Figure 8 and expanded vertically by a Gaussian distribution.

Since this light distribution is only a relative light distribution, the next step will be to find a suitable maximum for different driving velocities.

6. Discussion

To give some context to the data presented here, the allowed maximum luminous intensity in the U.S. is 75,000 cd per headlight or 150,000 cd per vehicle, showing that a driving speed of no more than 130 $\mathrm{km\,h^{-1}}$ is safe. For Europe, where the limit is at 215,000 cd per headlight, the maximum safe driving speed is around 155 $\mathrm{km\,h^{-1}}$, if such headlamps are equipped.

Of course, the headlight distribution shown in Figure 9 only works on perfectly straight roads with no distractions or other objects present along the road. Thus, such a light distribution would be absolutely unsuitable for real-world applications. Not only would drivers feel very uneasy due to a very limited amount of road illumination, but corners or other variations in road geometry outside an absolutely straight line would be very poorly illuminated. Under such conditions, even maintaining lateral position within one's lane might prove to be a difficult task. The distribution could only serve as a starting point for an approach to derive an optimal headlight distribution. However, as alluded to in the introduction to this publication, two papers will follow the present one. The second paper will focus on eye tracking and gaze distributions in real-life traffic in order to understand what drivers are actually focusing on. Of additional interest is the kind of road markings and parts of the light distribution that are used for orientation. The third paper will then focus on different road geometries and objects in the traffic space and will bring in the present and additional results from this paper and from the second paper in order to identify a headlight distribution that can also work in real-world driving.

Author Contributions: Conceptualization, J.K.; data curation, J.K.; formal analysis, J.K.; methodology, J.K.; software, J.K.; supervision, T.Q.K.; validation, J.K.; visualization, J.K. and A.E.; writing—original draft, J.K. and A.E.; writing—review and editing, J.K., A.E., J.D.B. and T.Q.K.; project administration, J.K. All authors have read and agreed to the published version of the manuscript.

Funding: This research received no external funding.

Institutional Review Board Statement: Not applicable.

Informed Consent Statement: Not applicable.

Data Availability Statement: All data generated or analyzed to support the findings of the present study are included in this article. The raw data can be obtained from the authors, upon reasonable request.

Acknowledgments: This article incorporates the results of the doctoral thesis submitted in 2018 to the Laboratory of Adaptive Lighting Systems and Visual Processing at the Technical University of Darmstadt, Germany, with the title "Optimization of Automotive Light Distributions for Different Real Life Traffic Situations" by Jonas Kobbert.

Conflicts of Interest: The authors declare no conflict of interest.

References

1. Bullough, J.D.; Liu, Y.W. Response to white light emitting diode aviation signal lights varying in correlated color temperature. *Transp. Res. Rec.* **2019**, *2673*, 667–675. [CrossRef]
2. Diem, C. Blickverhalten von Kraftfahrern im Dynamischen Straßenverkehr. Ph.D. Thesis, Technische Universität Darmstadt, Darmstadt, Germany, 2005.
3. Diem, C.; Schmidt-Clausen, H. Headlamp Performance in Traffic Situations. In Proceedings of the Symposium Progress in Automobile Lighting, PAL, Darmstadt, Germany, 23–24 September 1997; Volume 8.
4. Damasky, J.; Huhn, W. Variable Headlamp Beam Pattern—Lighting Requirements for Different Driving Situations. In *SAE Technical Paper*; SAE International: Warrendale, PA, USA, 1997.
5. Damasky, J.; Hosemann, A. The Influence of the Light Distribution of Headlamps on Drivers Fixation Behaviour at Nighttime. In *SAE Technical Paper*; SAE International: Warrendale, PA, USA, 1998.
6. Locher, J.; Völker, S.; Kleinkes, M.; Colin, I. Der Einfluss der Kfz-Lichtverteilung auf Sicherheit und Akzeptanz. In *Unpublished Manuscript LLAB Paderborn*; LLAB: Paderborn, Germany, 2002.
7. Kleinkes, M. Objektivierte Bewertung des Gütemerkmals Homogenität für Scheinwerfer-Lichtverteilungen. Ph.D. Thesis, Universität Bielefeld, Bielefeld, Germany, 2003.
8. Müller, N.; Waldner, M.; Bertram, T. Virtual Development and Optimization of High-Definition Headlights. In Proceedings of the 2022 International Conference on Electrical, Computer, Communications and Mechatronics Engineering (ICECCME), Malé, Maldives, 16–18 November 2022; pp. 1–6. [CrossRef]
9. Rosenhahn, E.O. Fog Headlamp-Visibility Investigations and Performance Requirements for Redefinition in Adaptive Headlamp Systems. In Proceedings of the SAE 2003 World Congress & Exhibition, Detroit, MI, USA, 3–6 March 2003. [CrossRef]
10. Rajesh Kanna, S.K.; Lingaraj, N.; Sivasankar, P.; Raghul Khanna, C.K.; Mohanakrishnan, M. Optimizing Headlamp Focusing Through Intelligent System as Safety Assistance in Automobiles. In *Advances in Manufacturing Technology*; Hiremath, S.S., Shanmugam, N.S., Bapu, B.R.R., Eds.; Springer: Singapore, 2019; pp. 533–545.
11. Erkan, A.; Hoffmann, D.; Kreß, N.; Vitkov, T.; Kunst, K.; Peier, M.A.; Khanh, T.Q. Required Visibility Level for Reliable Object Detection during Nighttime Road Traffic in Non-Urban Areas. *Appl. Sci.* **2023**, *13*, 2964. [CrossRef]
12. Reagan, I.J.; Brumbelow, M.L. Drivers' detection of roadside targets when driving vehicles with three headlight systems during high beam activation. *Accid. Anal. Prev.* **2017**, *99*, 44–50. [CrossRef]
13. Funk, C.; Vozza, A.; Petroskey, K. An Optimized Method for Mapping Headlamp Illumination Patterns. In *SAE WCX Digital Summit*; SAE International: Warrendale, PA, USA, 2021. [CrossRef]

14. Reagan, I.J.; Brumbelow, M.; Frischmann, T. On-road experiment to assess drivers' detection of roadside targets as a function of headlight system, target placement, and target reflectance. *Accid. Anal. Prev.* **2015**, *76*, 74–82. [CrossRef]
15. Reagan, I.J.; Frischmann, T.; Brumbelow, M.L. Test track evaluation of headlight glare associated with adaptive curve HID, fixed HID, and fixed halogen low beam headlights. *Ergonomics* **2016**, *59*, 1586–1595. [CrossRef]
16. Waldner, M.; Müller, N.; Bertram, T. Energy-Efficient Illumination by Matrix Headlamps for Nighttime Automated Object Detection. *Int. J. Electr. Comput. Eng. Res.* **2022**, *2*, 8–14. [CrossRef]
17. Cengiz, C.; Kotkanen, H.; Puolakka, M.; Lappi, O.; Lehtonen, E.; Halonen, L.; Summala, H. Combined eye-tracking and luminance measurements while driving on a rural road: Towards determining mesopic adaptation luminance. *Light. Res. Technol.* **2014**, *46*, 676–694. [CrossRef]
18. Winter, J.; Fotios, S.; Völker, S. The effect of assuming static or dynamic gaze behaviour on the estimated background luminance of drivers. *Light. Res. Technol.* **2019**, *51*, 384–401. [CrossRef]
19. Moisel, J. Adaptive Headlights Utilizing LED-Arrays. In Proceedings of the 8th International Symposium on Automotive Lighting (ISAL), München, Germany, 29–30 September 2009; Volume 13, pp. 287–296.
20. Economic Commission for Europe. *Uniform Provisions Concerning the Approval of Adaptive Front-Lighting Systems (AFS) for Motor Vehicles, Revision 2*; Technical Report; UN ECE: Geneva, Switzerland, 2013.
21. Sprute, J.H. Development of Lighting Engineering Criteria to Minimize the Glare of Adaptive High Beam Systems. Ph.D. Thesis, Technische Universität Darmstadt, Darmstadt, Germany, 2012.
22. Zydek, B. Blendungsbewertung von Kraftfahrzeugscheinwerfern unter dynamischen Bedingungen. Ph.D. Thesis, Technische Universität Darmstadt, Darmstadt, Germany, 2014.
23. Gibbons, R.; Terry, T.; Bhagavathula, R.; Meyer, J.; Lewis, A. Applicability of Mesopic Factors to the Driving Task. *Light. Res. Technol.* **2016**, *48*, 70–82. [CrossRef]
24. Bullough, J.; Skinner, N. Predicting stopping distances under different types of headlamp illumination. In Proceedings of the 8th International Symposium on Automotive Lighting, Darmstadt, Germany, 29–30 September 2009.
25. Hecht, S. The visual discrimination of intensity and the Weber-Fechner law. *J. Gen. Physiol.* **1924**, *7*, 235. [CrossRef]
26. Greibe, P. Determination of braking distance and driver behaviour based on braking trials. In Proceedings of the 87th Transportation Research Board Annual Meeting, Washington, DC, USA, 13–17 January 2008.
27. Damasky, J. Lichttechnische Entwicklung von Anforderungen an Kraftfahrzeug-Scheinwerfer. Ph.D. Thesis, Technische Hochschule Darmstadt, Darmstadt, Germany, 1995.
28. Brémond, R.; Bodard, V.; Dumont, E.; Nouailles-Mayeur, A. Target Visibility Level and Detection Distance on a Driving Simulator. *Light. Res. Technol.* **2013**, *45*, 76–89. [CrossRef]